Hindawi
Journal of Renewable Energy
Volume 2022, Article ID 4030369, 11 pages
https://doi.org/10.1155/2022/4030369

Research Article

Feasibility Study of a Hybrid PV/Hydro System for Remote Area Electrification in Rwanda

Emile Niringiyimana,[1] **Sun WanQuan**,[1] **and Giovanni Dushimimana**[2]

[1]*Renewable Energy and Clean Power, North China Electric Power University, Beijing, China*
[2]*Electrical Power Engineering and Its Automation, North China Electric Power University, Beijing, China*

Correspondence should be addressed to Emile Niringiyimana; nemile1988@gmail.com

Received 24 September 2021; Revised 20 May 2022; Accepted 31 May 2022; Published 24 June 2022

Academic Editor: Jedrzej Szmytkowski

Rwanda is among the least developed countries on the globe with total access to electricity not exceeding 63%, where the rest of the population lives in areas with no access to electricity. One such a place, which is the focus of this research, is Musanze district (1.4919 S, 29.5572 E), where 60% of the population in this area are located in remote areas, which makes the task of their electrification via grid system very difficult. Micro hydropower has been developed so far to reduce the deficit of energy access in this area. However, the power generated is not enough to cover the area, and the major problem is the decrease in river water level in the dry season, which affects the power generation. In this work, the feasibility of a hybrid PV/hydroelectric supply system is studied and optimized to increase the number of homes accessing electricity in this area. A 200 kW Mutobo micro hydro system in Musanze district under operation is considered a case study where a 100 kW PV array tied to the micro hydropower system is designed. The optimized PV-hydro hybrid system was proposed using a modified *P* and *O* MPPT algorithm to enhance the PV-generated power. The model was designed and simulated using MATLAB/Simulink, and data recorded from Mutobo micro hydropower station, Rwanda Energy Group, and National Meteorological Agency were used to estimate solar energy potentials. The results showed that the hybrid PV/hydro system is feasible and effectively contributes to the power shortage mitigation in remote areas during the dry season.

1. Introduction

Renewable energy source integration into grid systems (such as solar PV, hydro, and wind energy) is given higher significance with a higher depletion rate of fossil fuel resources. With the variation of solar and wind energy potential due to season, it is tough to increase the renewable energy portion of the grid. At the end of 2017, 26.5% of the power generated worldwide was electricity from renewable energy resources (RES), which has increased by 2% and jumped to 28.5% in 2020 according to the global energy reviews [1]. However, 17% of the population worldwide does not have access to electricity. More than 85% are living in rural areas, with sub-Sahara countries which occupy the largest percentage. Micro hybrid systems may be used as alternatives to the load supplied by nonrenewable energy sources such as diesel generators and coal with high efficiency, reliability, and high cost-effectiveness.

The combination of hybrid RES and conventional energy resources is more effective and cost-effective compared to single-source power systems. Presently, the total renewable power generation, including hydropower in Rwanda, is noticeably smaller than that of developed countries such as China, the United States, and Germany, which were 647 GW, 241 GW, and 112 GW, respectively, as of 2017 statistics. These countries invest a great amount of money in renewable energy as by 2019, it was $ 282.2 billion. This was a mere 1% higher than the total for the previous year, and it was 10% below the record figure of $ 315.1 billion set in 2017 [2].

Energy crisis is the main problem that Rwanda is facing and puts an obstacle to its development. Private sectors seem

to pay attention to energy sector development and increasing the power generation from renewable energy sources. Rwanda has the potential to integrate RES for continuous power supply, and they became a key for the national energy sector to increase energy access in the remote areas, but the power generation capacity of some plants is not enough in the dry season. Therefore, the complementary use of renewable energy such as solar PV power generation, wind power generation, and small hydropower generation as hybrid systems is the best technique to enhance the power generation and improve the local power supply without any conflict, available to everyone, environmentally friendly, reliable, and available at a cheap cost compared to other energy sources [3, 4].

2. Research Background

Many researches were conducted on the feasibility of hydro/solar/wind-based hybrid system. In paper [5], the authors proposed a yearly scheduling model of the hydro-PV-wind hybrid system, maximizing its generation power and considering the total firm power limits. In [6], integration and power control of a micro hydro-PV-wind-based hybrid microgrid was discussed, considering a hybridized generation according to the time-varying load. These systems improve the load factors, and the maintenance and replacement costs are reduced as the renewable resource devices complement each other.

For an optimal mixture of different renewable energy sources, researchers use various hybrid system optimization methods and some types of software, including linear programming, artificial intelligence, MATLAB/Simulink, and HOMER [7]. The authors in [8] discussed the feasibility of the hydro/PV/wind/diesel system using HOMER simulation software, and others in [8, 9] discussed the feasibility study and comparative analysis of hybrid renewable power system for off-grid. In [10], Yibo et al. designed a hydro/PV hybrid power system in an isolated microgrid. In paper [11], the authors discussed a novel topology for a standalone hybrid system with a combination of hydro and photovoltaic (PV). In [12], the authors designed a hydro-PV-wind-battery-diesel-based standalone hybrid power system using the HOMER software. The hybrid floating PV/hydropower plant was proposed by Niaki and Davoodi in [13], and simulations were performed using HOMER software. The authors in [14] used HOMER as the optimization tool and used the optimality ranking technique as a second method while determining the best optimal hybrid distributed generation system. A minihybrid power generation scheme consisting of a PV with a storage unit combined with a micro hydro generation unit and a diesel generator was proposed in southern Bangladesh [15]. The author discussed the economic viability with the technical aspects to set up such a system via HOMER analysis.

The traditional perturb and observe (*P* and *O*) MPPT is unsuitable for fast varying climate conditions because of its slow irradiance tracking ability with a fixed small perturbation value [16]. Plenty of studies about the use of hybrid systems were conducted in Rwanda. However, due to the lack of proper data collection, optimization methods, and use of old technology and devices in hydropower generation, the outcome of researches is still not enough to implement hybrid energy generation systems in Rwanda.

In this research, the optimized PV-hydro hybrid system is proposed using a new modified *P* and *O* MPPT algorithm to increase the PV-generated power with a reliable power control supplied to loads in remote area of Musanze small economic zone as declared by the government of Rwanda in 2016. The contribution of this research is as follows:

(a) The potential PV-hydro hybrid energy generation system application was investigated with an actual situation in the Musanze district as a case study.

(b) Standalone hybrid PV/micro hydro systems were developed to optimize the power generated and stabilize the energy supply to load demands.

(c) A new modified P and O MPPT algorithm was used, and the simulation was done in MATLAB.

(d) Analysis of results proved that the energy crisis in the remote areas could be mitigated by implementing standalone hybrid systems.

3. Materials and Methods

3.1. Data Collection. Every single component in PV-hydropower hybrid system needs to be designed. Some parameters were recorded from the Mutobo hydropower station, and the 240 SunPower SP-414E-WHT-D PV solar panel was selected from the PV module library in Simulink. The data in Tables 1 and 2 show the technical parameters and monthly weather data obtained from Musanze meteorological data observatory (1.4919 S, 29.5572 E), including hourly wind speed, hourly atmospheric temperature, hourly solar radiation, and hourly natural inflow over a year.

3.2. Load Profile Details. The proposed PV-hydro hybrid system considered 24 h load demand of a total of 500 households available in Mutobo village, 2 healthcare centers, 3 schools, and load forecasting for Musanze industrial zone. The load analysis for each household and healthcare facility usually consisted of refrigerators, fluorescent lamps, electric fans, TVs, and other small electric appliances.

3.3. System Design. The array system is composed of 66 parallel module strings and 5 series-connected 305.2 W solar panels that deliver a total maximum power of 100 kW at STC (800 W/m^2, 25°C), and the solar PV array output is connected to the system via a DC-DC boost converter, a three-phase three-level voltage source converter (VSC), and a transformer that adjust the AC power from VSC. The Maximum Power Point Tracking (MPPT) is implemented in the boost converter using a modified perturb and observe technique (*P* and *O*). The hydropower system in operation generates 200 kW power with plant parameters as described in Table 1.

Table 1: Technical information for Mutobo hydropower station.

Parameters	Values at Mutobo power station
Penstock length (m)	223
Hydraulic head H (m)	123.30
Designed flow rate 90% (m^3s^{-1})	0.932
Installed power capacity (kW)	200
Annual energy generation (MWh)	1749.8
Actual power potential ($\eta_o = 80\%$) (kW)	196
Turbine type	Francis
Turbine efficiency (%)	65

Table 2: Monthly meteorological data observatory for the selected village Mutobo [17].

Month	Clearness index	Daily radiation ($kWh/m^2/day$)	Wind speed (m/s)	Air temperature (°C)	Atmospheric pressure (kPa)	Relative humidity (%)
January	0.532	5.51	3.7	26	89.8	43.30
February	0.531	5.60	3.91	25.6	89.9	44.50
March	0.540	5.60	3.92	24.3	89.8	62.60
April	0.501	5.08	3.8	22.9	89.6	75.00
May	0.521	4.99	3.7	22.4	89.9	75.50
June	0.598	5.44	3.6	22.3	89.9	68.70
July	0.640	5.88	3.6	22.5	91	62.20
August	0.579	5.73	3.6	23	92	69.70
September	0.556	5.69	3.7	21.9	89.8	75.20
October	0.528	5.54	3.8	21.8	89.9	78.10
November	0.481	4.98	3.7	23	89.9	72.70
December	0.6	5.09	3.7	23.6	90	54.80

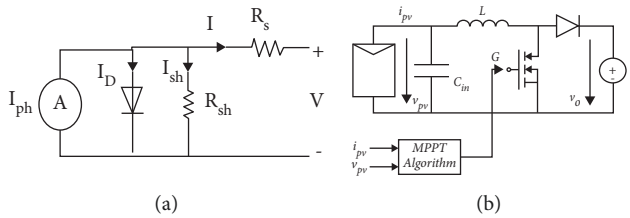

Figure 1: Solar PV basic circuits: (a) solar cell and (b) PV module.

3.3.1. Solar PV Array. The solar PV array is the combination of more than one PV module in parallel or series-connected systems.

Figures 1(a) and 1(b) show the basic equivalent circuit of the solar cell and PV module with the basic equation (1) used to calculate the generated current from the solar cell.

$$I = I_L - I_0\left[\text{Exp}\left\{\frac{q(V+R_s)}{akT}\right\} - 1\right] - \frac{(V+R_s)}{R_{\text{sh}}}, \quad (1)$$

where I is the cell o/p current, I_p is the photocurrent, I_d is the saturation current, q is the charge of an electron (1.6 e19 C), V is the PV cell output voltage, Rs is the series resistance, K is Boltzmann's constant (1.38 e23 J/K), T is the temperature (K), n is the ideality factor (1~2), and Rsh is the parallel resistance. The photocurrent is calculated in equation (2) [18] depending on solar irradiance and cell temperature.

$$I_p = -I_{\text{sc}} + K_t(T_c - T_r) \times \frac{H_r}{1000}. \quad (2)$$

As panels are of flat type with a lifetime of 2 years, the output of the PV array is calculated from the equation

$$P_{PV} = Y_{PV} f_{PV}\left(\frac{G_T}{G_{T,\text{STC}}}\right)\left[1 + \alpha_p\left(T_C - T_{C,\text{STC}}\right)\right], \quad (3)$$

where I_{SC} is the short-circuit current, K_i is the t^o coefficient, T_C is the cell temperature at STC, T_r is the cell ref t^o at STC, Hr is the solar Irr in W/m^2, Y_{pv} is the PV output power under STC, α_P is the temperature coefficient of power (%/°C), f_{PV} is the PV derating factor (%), $G_{T,\ STC}$ is the incident radiation under STC, and GT is the solar irradiation striking the PV panel (kW/m^2).

From equations (1) and (2), the PV model is modeled in MATLAB/Simulink, and the total array output power can be calculated from equation (3). The PV parameters behavior (current and power) are shown by the IV and PV characteristics curves in Figures 2(a) and 2(b) extracted at a different level of solar irradiances.

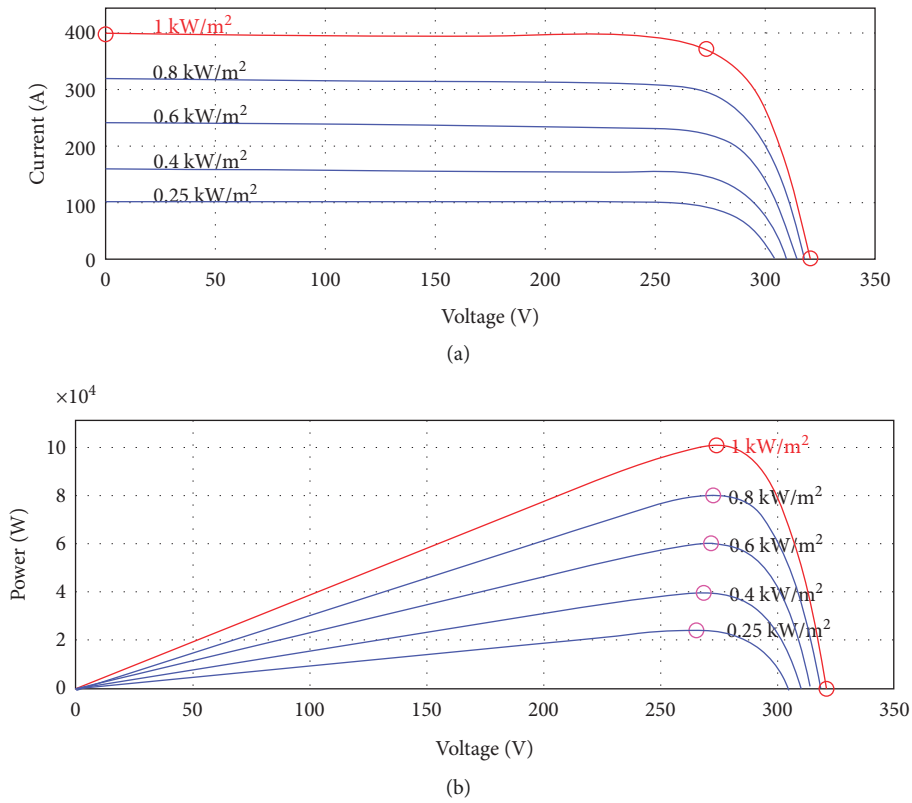

Figure 2: PV parameters behavior: (a) IV and (b) PV characteristics.

Table 3: PV array specifications for one module.

Parameters	Values
Number of series-connected cells	96
Open-circuit voltage (V_{oc})	64.2 V
Short-circuit current (I_{sc})	5.96 A
Voltage (V_{mp})	54.7 V
Current at maximum power (I_{mp})	5.58 A
Derating factor	75%

Table 3 shows the specifications of the PV module selected from the MATLAB library and used during the simulations.

The PV array system has two inputs in MATLAB/Simulink block that allows varying sun irradiance and temperature parameters in W/m^2 and in °C, respectively. The solar irradiance and temperature profiles are well-defined by a Signal Builder block which is connected to the PV array input terminals.

3.3.2. DC-DC Boost Converter. The boost converter is responsible for regulating PV outputs of interest and assuring convergence to the desired equilibrium point [19]. The boost converter in Figure 3 increases the system voltage from the PV natural voltage of 272 Vdc to 500 Vdc. The input-output voltage relationship of the booster converter can be denoted as a function of the duty cycle in equation (4) [20]. The duty cycle is adjusted by the perturb and observe-based MPPT controller, which automatically changes the duty cycle value to extract the required maximum power.

The duty cycle and the DC-DC boost converter are obtained by solving equation (4) [21]:

$$D = 1 - \frac{V_{\text{in}}(\min) \times \eta}{V_o},$$

$$1 - D = \frac{V_{\text{in}}(\min) \times \eta}{V_0}, \tag{4}$$

$$V_0 = \frac{V_{\text{in}}(\min) \times \eta}{1 - D},$$

where V_{in} is the input voltage to the DC-DC boost converter, V_{o} is the output voltage of the DC-DC boost converter, η is the converter efficiency, and c is the 3-level 3-phase voltage source converter (VSC).

A 3-level 3-phase voltage source converter converts the direct voltage to alternative voltage AC loads. The VSC

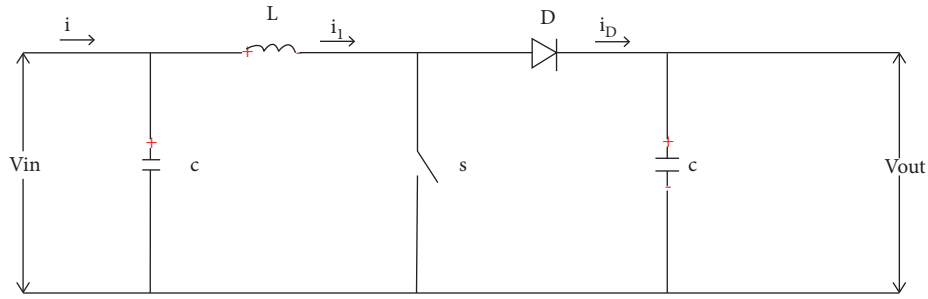

Figure 3: DC-DC boost converter.

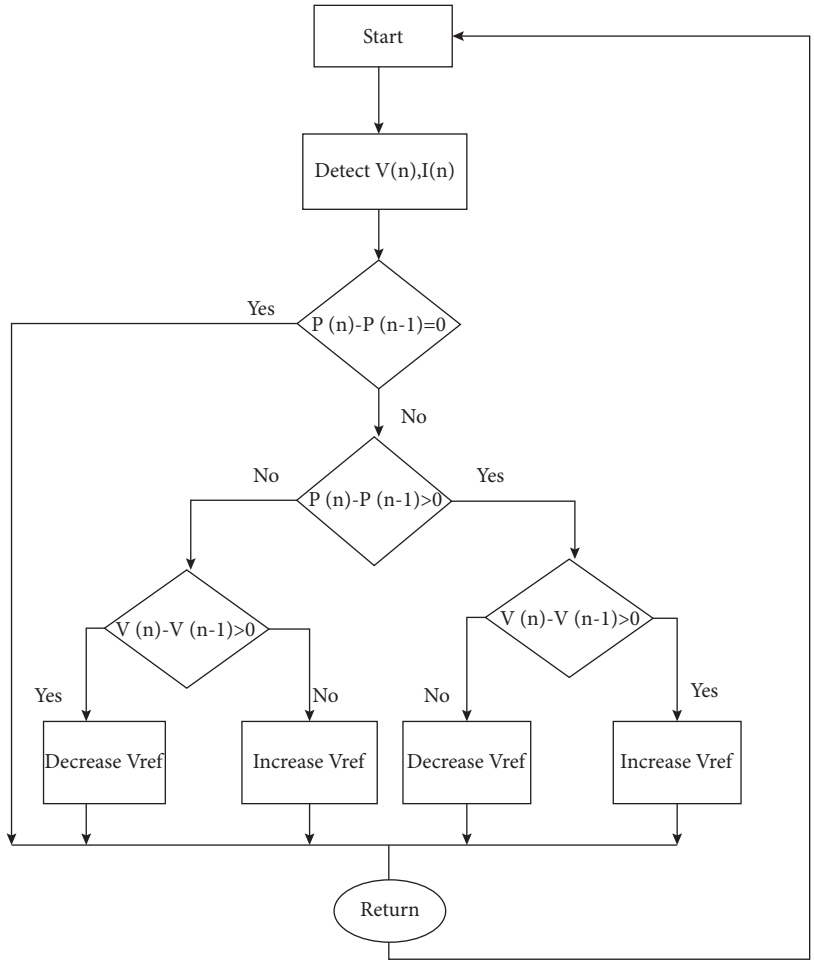

Figure 4: Perturb and observe algorithm.

converts 500 Vdc to alternative power that is transformed into the line voltage and keeps the unity power factor [4]. The VSC regulating system functions based on constant voltage and frequency control mode that controls voltage input to the load system. The VSC control system functions based on constant AC voltage and frequency control mode that regulates the output system voltage.

3.3.3. Perturb and Observe Algorithm. The *P* and *O* algorithm is also called the hill-climbing method. In this method, the MPPT method is based on the calculation of output power where the perturbation modifies the output power of the PV system. The voltage is increased when the perturbation increases towards the maximum power point, and when the perturbation decreases, the voltage also must be decreased. The duty cycle also changes, and the procedure lasts as long as the maximum power point is not reached [22]. The perturb and observe MPPT algorithm is implemented in the MPPT Control MATLAB Function block to maximize the solar irradiance.

Figure 4 shows the flowchart of *P* and *O* algorithm. Firstly, the values of *V(n)* and *I(n)* are determined. Then, the derivative of generated power (dP/dV) is checked at three

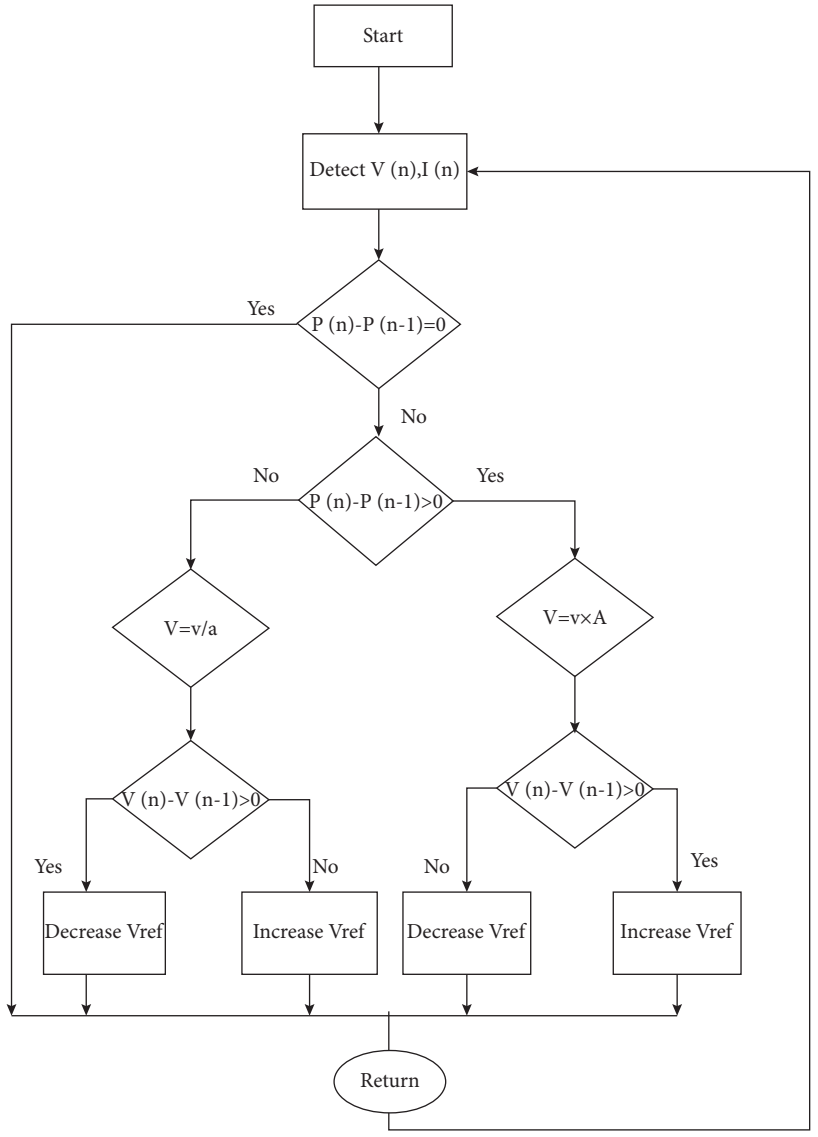

Figure 5: Modified perturb and observe algorithm.

different conditions referring to the position of MPP [23] as follows:

(a) The derivative dP/dV = 0 is at the same point with the MPP.

(b) The derivative dP/dV > 0 is at the left of MPP, which means that the derivative of PV characteristic is greater than zero and located to the left of the MPP and less than zero and located to the right of the MPP.

(c) The derivative dP/dV < 0 of the PV characteristic is at the right side of the MPP.

3.3.4. Hydropower System. The run-of-river hydro turbine was considered for the research, and the power calculation is shown in equation (4). In nominal conditions, the available head (h), the penstock length, and the design flow rate (Q_{design}) are 123.3 m, 223 m, and 0.932 m^3/s, respectively, which results in the nominal hydropower of 200 kW. The nominal hydropower (P_{hyd}, nom) is calculated in equation (5) as follows:

$$P_{hy\ d,nom} = \frac{\eta_{hy\ d} \cdot \rho_{hy\ d} \cdot g.h.Q_{de\ sign}}{1000}, \quad (5)$$

where η_{hyd} is the hydro turbine efficiency considered to be 65%, ρ is the water density (1000 kg/m^3), and g is the gravity acceleration (9.81 m/s^2). The HPP variable parameter for sensitivity study is the available head, which is equal to 123.3 m, 122 m, and 120 m, considering its changes in different seasons of the year.

4. Proposed System

4.1. System Description. The PV modules, DC-DC boost converter, the MPPT, and the VSC in Figure 5 are all modeled in Simulink. The block diagram of the proposed 3-level 3-phase VSC converts the generated voltage to AC. In

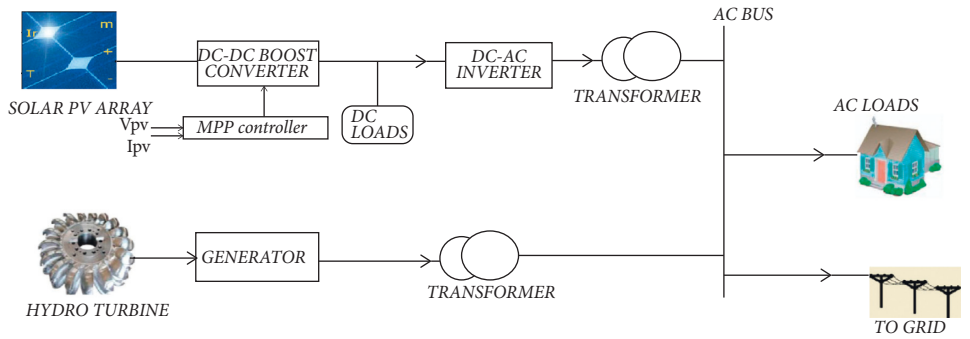

(a)

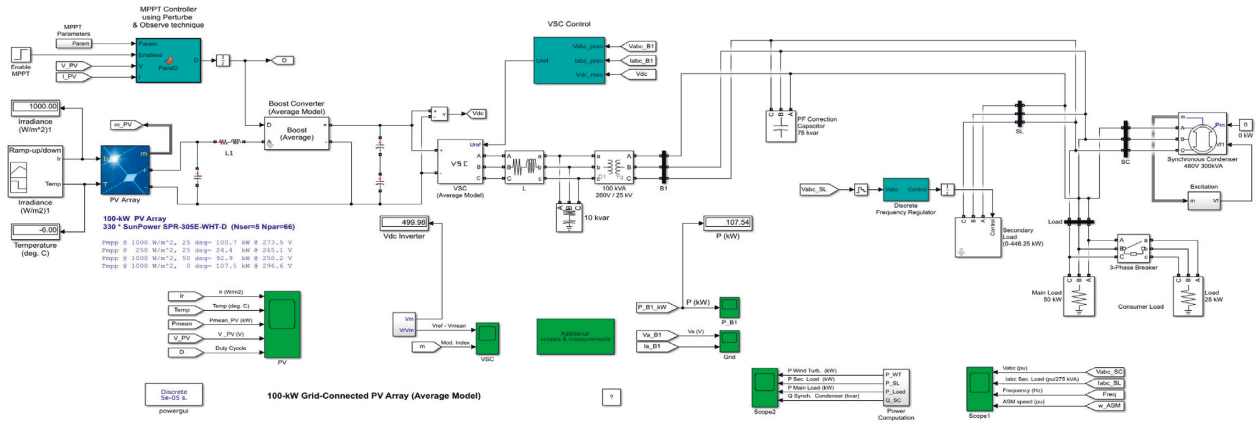

(b)

Figure 6: Proposed 100 kW PV system connected to Mutobo hydropower: (a) block diagram and (b) Simulink model.

this system, a three-level, neutral point connection inverter is used as the power electronic interface between the PV system and the hydro grid system. The boost converter and VSC converters are represented by equivalent voltage sources in this model generating the AC voltage averaged over one cycle of the switching frequency. In such a model, harmonics are not represented, but the dynamics resulting from control system and power system interaction are preserved. From this model, a much larger time step is used than the detailed model (50 microseconds versus 1 microsecond), resulting in a much faster simulation.

4.2. Methodology

4.2.1. Framework. The operation of hybrid system under different size of solar and hydropower plants is simulated, and results are analyzed based on which the optimal size of a PV plant integrated into a micro hydropower plant could be determined. Figure 6(a) is the schematic framework of the study. The PV and micro hydropower are developed based on their unique features to simulate the operation of hybrid systems under various sizes. The designed model aims to optimize the daily power generated from the hybrid system using a solar PV embedded MPPT with a modified *P* and *O* optimization algorithm.

Table 4: Parameter used for modified perturb and observe.

V_{PV}	PV voltage
I_{PV}	PV current
P_{PV}	PV power
ΔV	Change of voltage
ΔP	Change of power
V	Step size
a	Constant
V_{mpp}	Voltage at mpp

The complementarity of power generated from PV modules and hydropower is done when the energy from hydro is decreased; otherwise, the energy generated from PV modules is stored. The solar panels generate the maximum power even when the sun irradiance decreases, especially on cloudy days.

4.2.2. Modified P and O Algorithm. The parameters used in the modified perturb and observe algorithm (*P* and *O*) are shown in Table 4. Those parameters were used to modify the algorithm.

P and *O* in Figure 4 show how the global MPP is tracked under irradiance decrease. The system measures the solar module V_{PV} and current I_{PV}. Then, the MPP tracking process starts with calling the *P* and *O* algorithm routine.

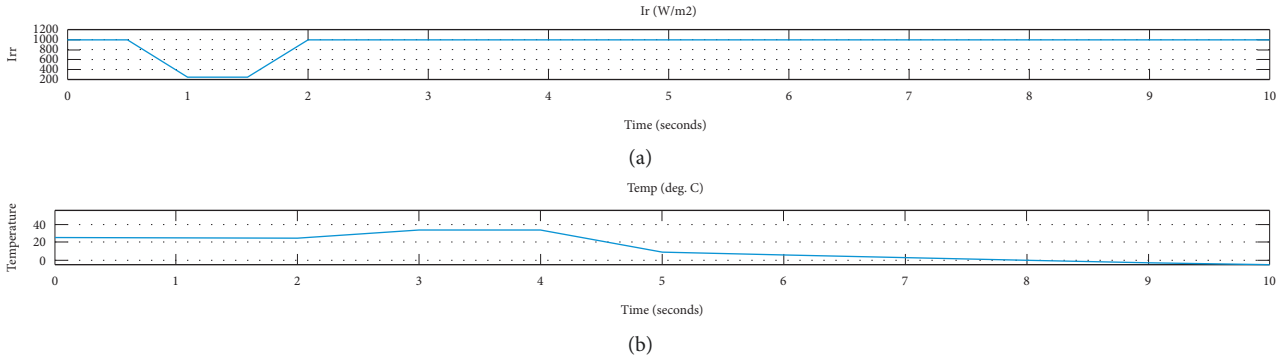

Figure 7: Environment conditions: (a) solar PV array input irradiance and (b) module temperature.

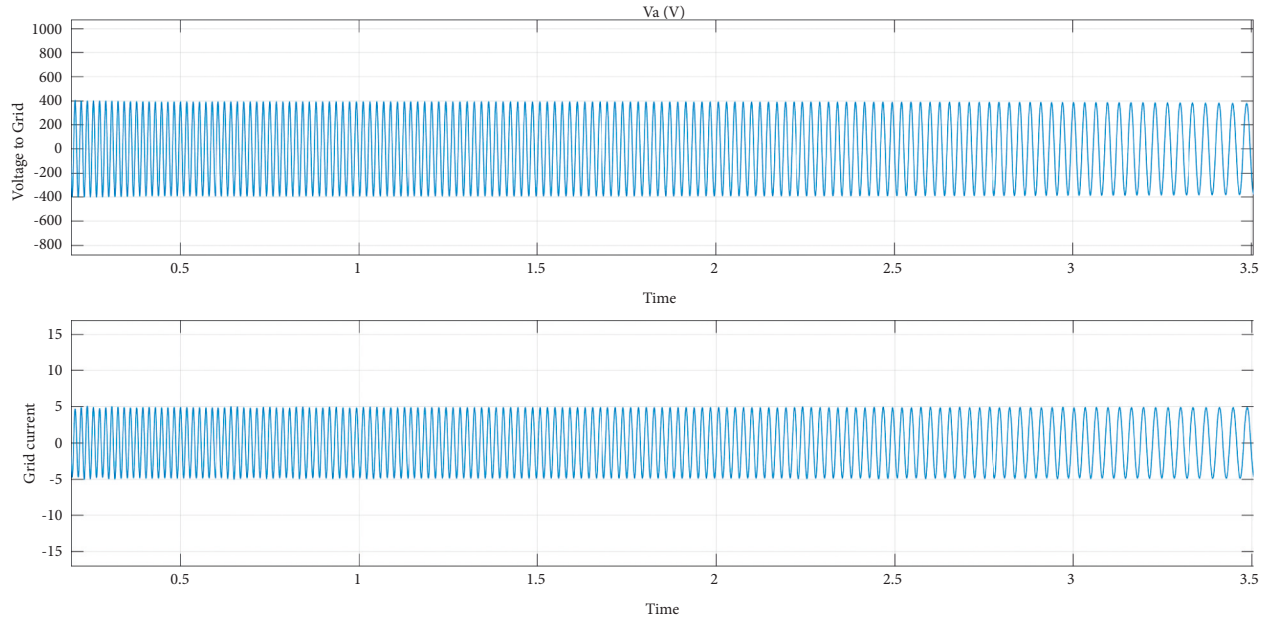

Figure 8: System outputs with modified P and O method: system voltage and current.

The modified P and O algorithm is proposed in Figure 5. When the perturbation is towards the MPP, the step size is increased by multiplying the step size V with a constant "a" when $\Delta P > 0$. Otherwise, the step size V is divided with a constant "a" to have a smaller step size as the sign of perturbation becomes negative $\Delta P > 0$. The constant "a" must be greater than 1 to increase the track speed as well as having a more accurate value of MPP.

4.3. Block Diagram of the Proposed System and MATLAB/Simulink Model. Figures 6(a) and 6(b) show the detailed block and Simulink diagrams, respectively, of the proposed PV-hydro hybrid system.

5. Simulation and Results

5.1. MATLAB Simulation

5.1.1. PV Array Output. Figure 7 shows the environment conditions, and the system runs at the standard test conditions (STC: 25°C and 1000 W/m^2, temperature and irradiance, resp.). The duty cycle is constant from time $t = 0$ sec to time $t = 0.3$ sec ($D = 0.5$). The output voltage is calculated $V = (1 - D)$ *Vdc. The mean PV output power is 96 kW, whereas the specified maximum power at STC is 100.7 kW. From Figure 8, the voltage and current are in phase. The MPPT is enabled at time $t = 0.3$ sec; therefore, the MPPT regulator starts regulating the PV voltage by varying the duty cycle in order to extract the maximum power generated from the PV. The maximum power is obtained at the duty cycle $D = 0.453$.

From time $t = 0.3$ sec to time $t = 0.5$ sec, the array operates at STC, and the duty cycle D value varies between 0.450 and 0.459. The PV array generated the outputs (voltage and power), which are calculated in formula (6) and 75 voltage, respectively.

$$V_{\mathrm{PV}} = N_{\mathrm{ser}} \times V_{\mathrm{mp}}. \tag{6}$$

$V_{PV} = 5 \times 54.7 = 273.5\,V$. The generated 273.5 V PV voltage, as shown in Figure 9(b), is later regulated to 500 V

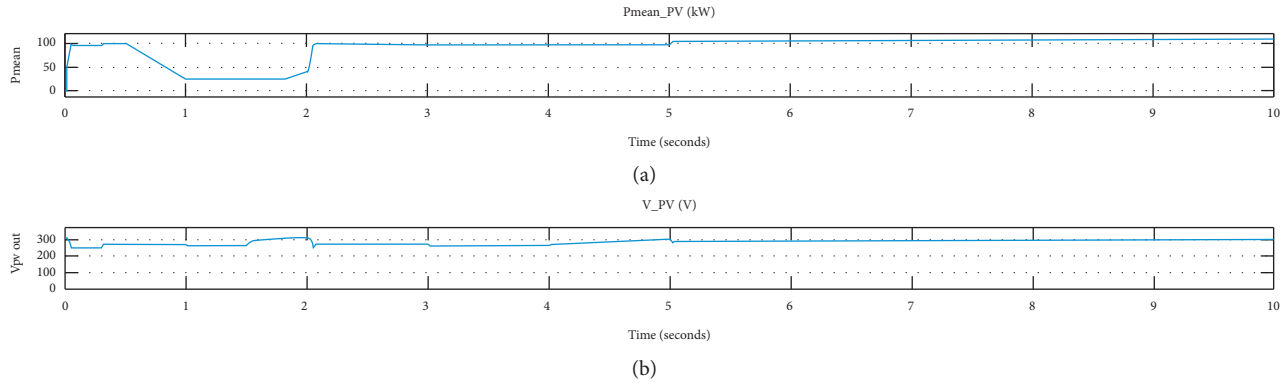

Figure 9: PV array outputs: (a) array generated power output and (b) array voltage output.

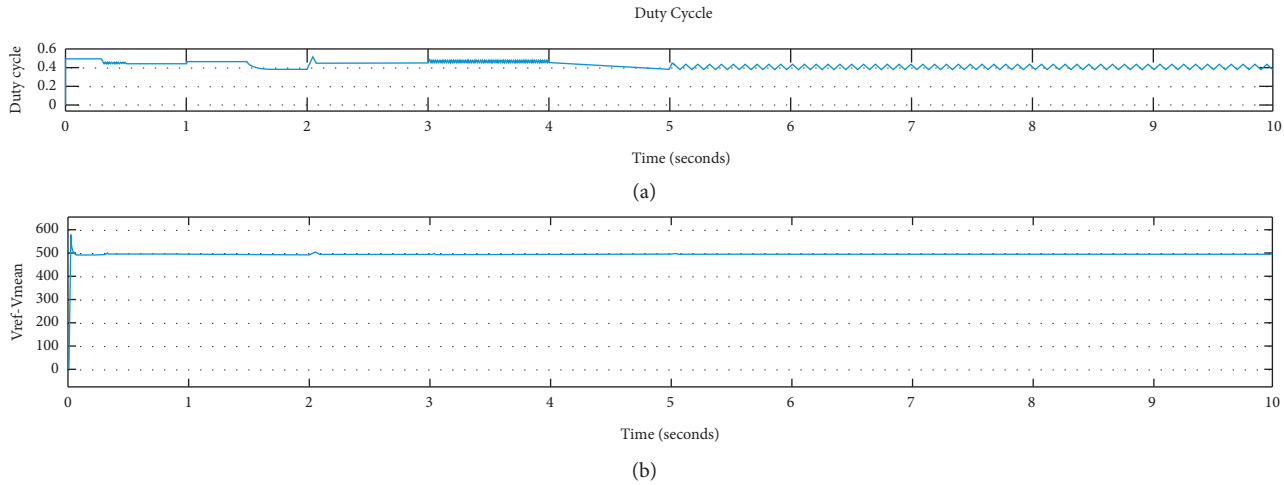

Figure 10: DC-DC boost converter: (a) duty cycle and (b) output voltage.

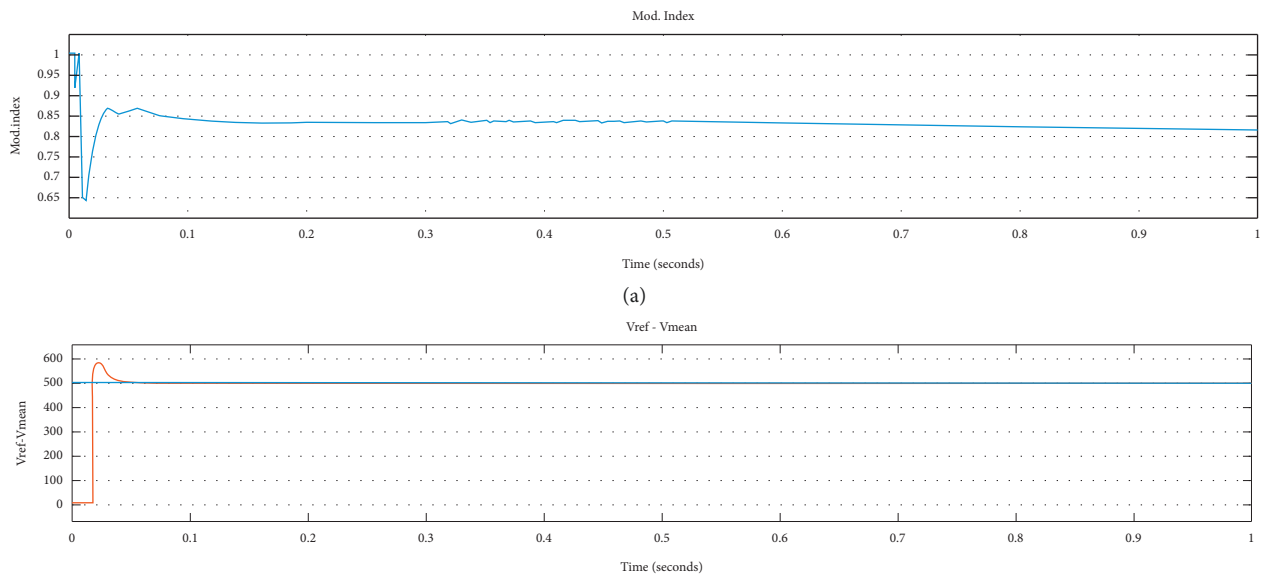

Figure 11: VSC outputs: (a) modulation index and (b) V_{ref}-V_{mean}.

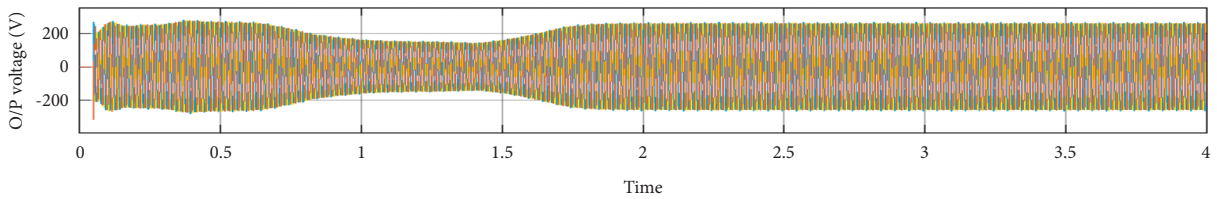

Figure 12: PV array output with traditional P and O method.

by varying the duty cycle by the DC-DC converter, and the obtained results are shown in Figure 10(b).

The VSC in Figure 11 converts the output of the DC-DC converter, the alternating current, and voltage to AC; the power generated is calculated in equation (5).

$$P_{\mathrm{PV(out)}} = V_{\mathrm{PV}} \times I_{\mathrm{PV}}. \tag{7}$$

I_{PV} is the total string current.

$$P_{\mathrm{PV(mean)}} = 273.5 \times (66 \times 5.58). \tag{8}$$

P_{PV} (out) = 100.7 Kw, as expected from the PV array simulation in Figure 9(a).

As the irradiance is ramped down at 0.5th sec to 1st sec, from 1000 W/m^2 to 250 W/m^2 as shown in Figure 7(a), the PPT controller tracks maximum power only, while irradiance stays constant. When the irradiance stays at 250 W/m^2 and the duty cycle value increases from 0.466 to 0.473, the PV voltage and power also decrease to 265 V and 24.4 kW, respectively, as in Figures 9(a) and 9(b). Figures 10(a) and 10(b) show the output duty cycle and the output voltage of the DC-DC boost converter, respectively.

From $t = 1.5$ sec to $t = 6.0$ sec, sun irradiance is restored back to 1000 W/m^2, and then the temperature is varied between 20 and 5°C. This shows the impact of temperature on the output of the PV module when environment condition changes, especially temperature and irradiance. The desired maximum PV output power (107.5 kW) is obtained from the 2 sec to 10 sec when the irradiance is at maximum and when the temperature is decreased to 5°C, as shown in Figure 7(a).

The basic principle of the P and O algorithm used in previous studies is the use of an extra checking condition ΔI in the traditional P and O algorithm to avoid the drift. From simulations results, as shown in Figure 7(a), the modified P and O algorithm-based MPPT tracks the maximum solar irradiance under varying module temperature, as shown in Figure 7(b), regardless of how fast the climatic conditions are changing with a great perturbation value compared to the traditional P and O.

From the simulation results, Figure 8 describes the system output voltage and current injected into the grid line to supply the local load. It is demonstrated that the new algorithm is much faster and more accurate than the traditional P and O method compared to Figure 12 of the traditional P and O algorithm. The voltage output of the modified P and O algorithm in Figure 8 converges more rapidly to MPP between 0.5 sec to 1.5 sec intervals of time when irradiance decreases compared to the traditional P and O algorithm. The output power, voltage, and current performance of the proposed method and P and O method when the irradiation changes are illustrated in Figure 9. Compared to other hybrid systems such as micro hydro/diesel, PV/micro hydro battery/diesel, and PV/hydro/wind hybrid systems, the proposed hybrid system is more environmentally friendly, easy to operate, and competitive in terms of energy cost-effectiveness and maintenance cost.

6. Conclusion

In this paper, the hybrid system introduced above is based on available renewable energy sources in northern Rwanda. The system combines the run-of-river hydropower station together with a PV power generation working in parallel mode through the parallel control strategies of inverter. The basic principle of the P and O algorithm is to use an extra checking condition ΔI in the traditional P and O algorithm to avoid the drift.

The PV-generated power is free from drift and is accurately tracking the maximum power from the PV panel. The system consists of the PV array as a source of power to be tied to a 200 kW Mutobo micro hydropower to supply the local load nearby. The proposed model uses a modified P and O algorithm-based MPPT, which is suitable for the fast varying of climate conditions due to its fast solar irradiance tracking ability with a great perturbation value compared to the traditional (P and O). The peak power (107 kW) is captured at a maximum solar irradiance. Results showed that the proposed system can be integrated into the grid and satisfies the load supply, especially during the dry season when the river water level decreases and the solar irradiance is at maximum. The proposed modified algorithm improves the generation of the PV system by gaining the extra power during drift, and this makes it more efficient compared to the traditional P and O algorithm. Compared to other energy sources combinations such as micro hydro/diesel, PV/micro hydro battery/diesel, and PV/hydro/wind hybrid system, this work demonstrated that the PV-hydro hybrid system using modified P and O MPPT technique is feasible, reliable, more environmentally friendly, and competitive in terms of cost-effectiveness, maintenance, and energy cost.

Data Availability

The data provided are recorded directly from the research site. There is no specific link or website for data used in this project.

Conflicts of Interest

The authors declare that they have no conflicts of interest.

Acknowledgments

This work was supported by the National Key Research and Development Project (2016YF0401900).

References

[1] J.-B. Zakia Adam, H. Bahar, C. Barret et al., *Global Energy Review 2020, The Impacts of the Covid-19 Crisis on Global Energy Demand and CO_2 Emissions*, International Energy Agency (IEA), Paris, France, 2020.

[2] A. McCrone, *Global Trends in Renewable Energy Investment 2020*, Frankfurt School FS UNEP Collaborating Center for Climate Sustainable Energy Finance, Germany, 2020.

[3] Z. Yang, C. Wu, H. Liao, Y. Wang, and H. Wang, *Research on Hydro/Photovoltaic Hybrid Generating System*, IEEE, Piscataway, NJ, USA, 2010.

[4] S. Wanquan, E. Niringiyimana, P. Simiyu, V. Ndayishimiye, and G. Dushimimana, *Modelling a 30°kW Standalone Solar Powered Irrigation System*, IEEE PES/IAS PowerAfrica, Hyderabad, India, 2020.

[5] Y. Liu, S. Tan, C. Jiang, and N. Q. Nv, "Interval optimal scheduling of hydro-Pv-wind hybrid system considering total firm power coordination," in *Proceedings of the International Conference on Renewable Power Generation*, Beijing, China, 2015.

[6] S. Pati, *Integration and Power Control of a Micro-Hydro-PV-Wind Based Hybrid Microgrid*, IEEE, Piscataway, NJ, USA, 2017.

[7] G. Bekele and G. Tadesse, "Feasibility study of small hydro/PV/wind hybrid system for off-grid rural electrification in Ethiopia," *Applied Energy*, vol. 97, pp. 5–15, 2012.

[8] J. O. Oladigbolu, M. A. M. Ramli, and Y. A. Al-turki, "Feasibility study and comparative analysis of hybrid renewable power system for off-grid rural electrification in a typical remote village located in Nigeria," *IEEE Access*, vol. 8, pp. 171643–171663, 2020.

[9] L. Al-Ghussain, H. Ahmed, and F. Haneef, "Optimization of hybrid PV-wind system: case study Al-Tafilah cement factory, Jordan," *Sustainable Energy Technologies and Assessments*, vol. 30, pp. 24–36, 2018.

[10] W. Yibo, I. Member, and X. Honghua, "Research and practice of designing hydro/photovoltaic hybrid power system in Microgrid," *IOP Conference Series Materials Science and Engineering*, vol. 180, pp. 1509–1514, 2013.

[11] M. Rezkallah, S. Sharma, and A. Chandra, *Hybrid Standalone Power Generation System Using Hydro-PV-Battery for Residential Green Buildings*, IEEE, Piscataway, NJ, USA, 2015.

[12] M. M. A. Rahman and A. T. Al Awami, *Hydro-PV-Wind-Battery-Diesel Based Stand-Alone Hybrid Power System*, IEEE, Piscataway, NJ, USA, 2014.

[13] A. H. M. Niaki and B. Davoodi, *Proposing an Optimal Techno-Economic Scheme for a Hybrid Floating Photovoltaic-Hydro Power Plant*, IEEE, Piscataway, NJ, USA, 1957.

[14] S. Twaha and M. U. Mukhtiar, *Optimal Hybrid Renewable-Based Distributed Generation System with Feed-in Tariffs and Ranking Technique*, IEEE, Piscataway, NJ, USA, 2014.

[15] H. S. Das, A. H. M. Yatim, C. W. Tan, and K. Y. Lau, "Proposition of a PV/tidal powered micro-hydro and diesel hybrid system: a southern Bangladesh focus," *Renewable and Sustainable Energy Reviews*, vol. 53, pp. 1137–1148, 2016.

[16] S. Sheik Mohammed, D. Devaraj, and T. P. Imthias Ahamed, "A novel hybrid maximum power point tracking technique using perturb and observe algorithm and learning automata for solar PV system," *Energy*, vol. 112, pp. 1096–1106, 2016.

[17] H. G. Beyer and J. Uwibambe, "Design of photovoltaic system for rural electrification in Rwanda," *Journal of Energy Research and Review*, vol. 7, 2017.

[18] S. Dorji, D. Wangchuk, T. Choden, and T. Tshewang, "Maximum power point tracking of solar photovoltaic cell using Perturb and observe and fuzzy logic controller algorithm for boost converter and quadratic boost converter," *Materials Today Proceedings*, vol. 27, pp. 1224–1229, 2020.

[19] G. Gkizas, "Control engineering practice optimal robust control of a cascaded DC—DC boost converter," *Control Engineering Practice*, vol. 107, Article ID 104700, 2021.

[20] G. Singh and S. Kundu, "An efficient DC-DC boost converter for thermoelectric energy harvesting," *International Journal of Electronics and Communications*, vol. 118, pp. 153–132, 2020.

[21] S. Palanidoss, *Experimental Analysis of Conventional Buck and Boost Converter with Integrated Dual Output Converter*, IEEE, Piscataway, NJ, USA, 2017.

[22] A. Nigam and A. K. Gupta, *Performance and Simulation between Conventional and Improved Perturb and Observe MPPT Algorithm for Solar PV Cell Using MATLAB/Simulink*, IEEE, Piscataway, NJ, USA, 2016.

[23] S. Bandri, Zulkarnaini, A. Syofian, and A. Effendi, "The application of perturb and observe algorithm to optimized of solar cell output the application of perturb and observe algorithm to optimized of solar cell output," in *Proceedings of the 2018 International Conference on Research and Learning of Physics*, p. 1185, Marmaris, Turkey, 2019.